

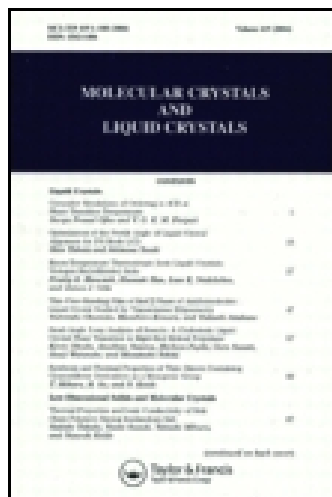
This article was downloaded by: [Florida Atlantic University]

On: 13 November 2014, At: 17:00

Publisher: Taylor & Francis

Informa Ltd Registered in England and Wales Registered Number: 1072954

Registered office: Mortimer House, 37-41 Mortimer Street, London W1T 3JH, UK



Molecular Crystals and Liquid Crystals

Publication details, including instructions for authors and subscription information:

<http://www.tandfonline.com/loi/gmcl20>

Synthesis and Thermal Properties of Twin Dimers Containing Cyanostilbene Derivatives as a Mesogenic Group

T. Mihara^a, M. Ito^a & N. Koide^a

^a Department of Chemistry, Faculty of Science, Science University of Tokyo, 1-3 Kagurazaka, Shinjuku-ku, Tokyo, 162-8601, Japan

Published online: 18 Oct 2010.

To cite this article: T. Mihara, M. Ito & N. Koide (2004) Synthesis and Thermal Properties of Twin Dimers Containing Cyanostilbene Derivatives as a Mesogenic Group, *Molecular Crystals and Liquid Crystals*, 419:1, 69-86, DOI: [10.1080/15421400490478326](https://doi.org/10.1080/15421400490478326)

To link to this article: <http://dx.doi.org/10.1080/15421400490478326>

PLEASE SCROLL DOWN FOR ARTICLE

Taylor & Francis makes every effort to ensure the accuracy of all the information (the "Content") contained in the publications on our platform. However, Taylor & Francis, our agents, and our licensors make no representations or warranties whatsoever as to the accuracy, completeness, or suitability for any purpose of the Content. Any opinions and views expressed in this publication are the opinions and views of the authors, and are not the views of or endorsed by Taylor & Francis. The accuracy of the Content should not be relied upon and should be independently verified with primary sources of information. Taylor and Francis shall not be liable for any

losses, actions, claims, proceedings, demands, costs, expenses, damages, and other liabilities whatsoever or howsoever caused arising directly or indirectly in connection with, in relation to or arising out of the use of the Content.

This article may be used for research, teaching, and private study purposes. Any substantial or systematic reproduction, redistribution, reselling, loan, sub-licensing, systematic supply, or distribution in any form to anyone is expressly forbidden. Terms & Conditions of access and use can be found at <http://www.tandfonline.com/page/terms-and-conditions>

SYNTHESIS AND THERMAL PROPERTIES OF TWIN DIMERS CONTAINING CYANOSTILBENE DERIVATIVES AS A MESOGENIC GROUP

*T. Mihara, M. Ito, and N. Koide**

*Department of Chemistry, Faculty of Science,
Science University of Tokyo, 1-3 Kagurazaka,
Shinjuku-ku, Tokyo 162-8601, Japan*

We synthesized twin dimers (TDs) with different linking groups between a mesogenic group and a flexible spacer, different spacer length, and different terminal alkyl chain length to clarify the effect of these groups on the mesomorphic properties of the TDs. A remarkable odd–even effect on the phase transition temperatures and nematic–isotropic phase transition entropy changes was observed for the TDs with different spacer length. Liquid crystallinity of TDs with ester linking group was superior to that of TDs with ether linking group. Length of terminal group played an important role in exhibiting a smectic phase for TDs with ester linking group.

Keywords: cyanostilbene; odd–even effect; liquid crystal dimer

INTRODUCTION

Main-chain-type liquid crystalline polymers (MCLCPs) with wholly aromatic rings and semirigid moieties have been found primarily as high-performance polymers for molding resins with good mechanical properties. MCLCPs can be classified into three types, Xyder, Vectra, and X7G, depending upon their heat distortion temperatures. The chemical constituents of semirigid MCLCPs like X7G have consisted of the mesogenic core and flexible spacer. Consequently, semirigid MCLCPs had lower phase transition temperatures than wholly aromatic MCLCPs, and thus semirigid MCLCPs can easily exhibit mesophases in the wide temperature range. Therefore many academic researchers have synthesized semirigid MCLCPs to clarify the relationship between their chemical structures and thermal properties [1].

*Corresponding author. E-mail: nkoide@ch.kagu.sut.ac.jp

Thermal properties of semirigid MCLCPs were dependent upon the chemical structure of the mesogenic core, flexible spacer length, the linking group between the mesogenic core and flexible spacer, etc. The odd–even effect is well known for the MCLCPs with different flexible spacer length. The odd–even effect is as follows: nematic–isotropic phase transition temperature and entropy changes from a nematic phase to an isotropic phase change alternately with the number of methylene units in the flexible spacer. The odd–even effect would be explained by the different orientational order of the mesogenic groups in a nematic phase, depending upon the number of methylene units with all-trans conformation in the flexible spacer.

The clear odd–even effect on the transition temperatures and entropy changes for the nematic–isotropic phase transition was observed for the semirigid MCLCPs, as shown in Figure 1. Thus, the odd–even effect had thermodynamic properties very familiar to the semirigid MCLCPs. Low molecular weight model compounds having structural units constituting the semirigid MCLCP offer good information on the odd–even effect on the phase transition temperatures, as well as entropy changes of the semirigid MCLCPs by experimental and computer simulation techniques [2,3]. There are two types of model compounds. One is a core model that had a single mesogenic core with two terminal chains. Another is a twin dimer (TD) model in which two mesogenic cores are linked by a flexible spacer.

TDs are recognized as an exact structural model compound of semirigid MCLCPs [2]. Abe and Furuya have found that the different orientation of each mesogenic group in the nematic phase played an important role for the odd–even effect on the nematic–isotropic phase transition behavior of the TD by the conformation analysis of the flexible spacer [3]. Moreover, TDs are recognized as interesting materials themselves, as well as the structural model of the semirigid MCLCPs [4–6]. The symmetric Schiff's base dimers were found to exhibit a smectic polymorphism [7]. Symmetric and nonsymmetric dimers consisting of the azobenzene mesogenic group were also investigated. The spacer length had a profound influence on the clearing temperatures of these dimers. A remarkable odd–even effect on the transition temperatures and entropy changes for the

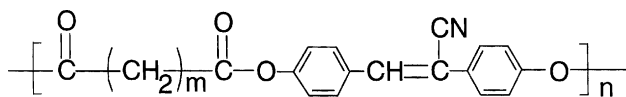


FIGURE 1 Chemical structure of main-chain liquid crystalline polymer containing cyanostilbene moieties.

mesomorphic–isotropic transition was observed for the dimer series. The thermal stability of a smectic A phase exhibited by the dimer series increased with increasing terminal chain length but decreased with increasing spacer length [8].

Hogan et al. and Attard et al. reported thermal properties of nonsymmetric dimers with different mesogenic groups such as cyanobiphenyl and alkylanilinebenzylidene [9,10]. The reports proposed that novel phases involving intercalated smectic phases stabilized by the mixed mesogenic group interaction. The magnitude of the odd–even effect was a sensitive function of the geometry of the linking group between the flexible alkyl chain and the mesogenic groups [4,5,11].

Watanabe et al. reported that the smectic layered structures of α , ω -bis(4,4'-butoxybiphenyl-carboxyloxy) alkanes was dependent upon the number of carbon atoms in the flexible spacer [12]. The authors found that the dimers with an even number of methylene units in the alkyl spacer formed a smectic A phase and that the dimers with an odd number of methylene units in the alkyl spacer formed a bilayer smectic C₂ phase. The orientation of the mesogenic groups was controlled by the conformation of the flexible spacer. The authors also reported that the achiral TD formed antiferroelectric smectic liquid crystal [13]. The exhibition of the antiferroelectric smectic phase would be controlled by the alkyl spacer conformation and the linking group.

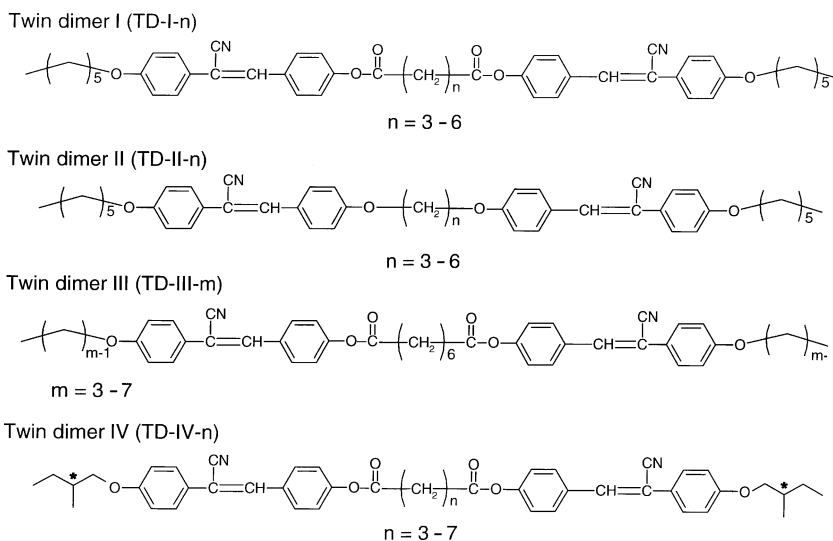


FIGURE 2 Chemical structures of twin dimers containing cyanostilbene derivatives.

We reported synthesis and thermal properties of TD having cyanostilbene moieties as a mesogenic group [14]. In the report, we discussed the relationship between the mesomorphic properties and the linking group between the flexible spacer and the mesogenic group, and found that the linking group played an important role for the exhibition of mesophase.

In this report, we synthesized TDs having the cyanostilbene moieties with different terminal chains or different flexible spacer lengths as shown in Figure 2, and investigated thermal properties of the dimers with different linking group or different terminal group.

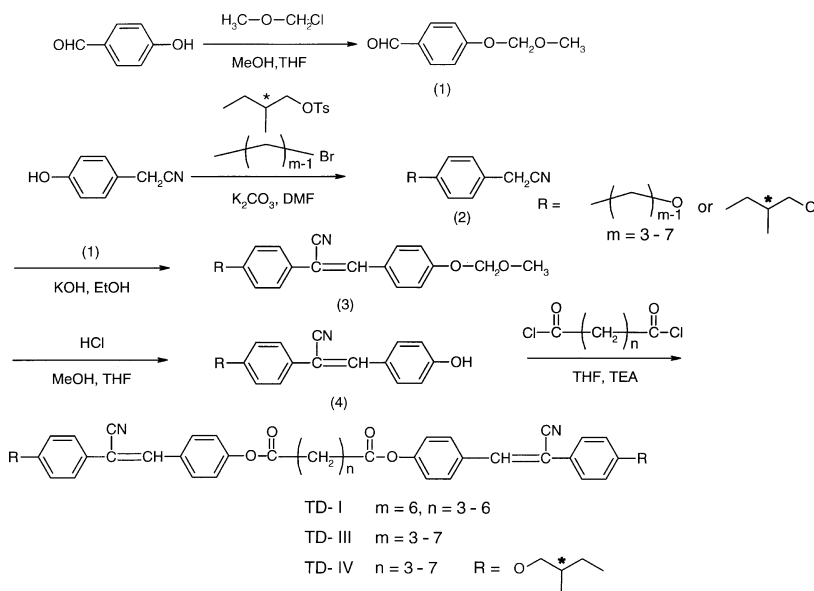
EXPERIMENTAL

Materials

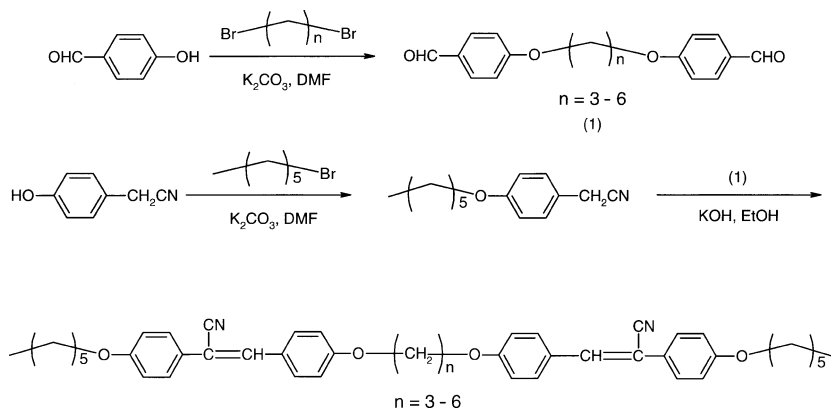
4-Methoxyphenyl acetonitrile was purchased from Midorikagaku corporation (Tokyo). TDs were prepared according to Schemes 1 and 2, respectively. Typical synthetic procedures were described below.

4-Formylphenylmethoxymethylether(1)

Diisopropylamine (10.7 g, 147.0 mmol) was added to a tetrahydrofuran solution (10 ml) of p-hydroxybenzaldehyde (6.2 g, 49.0 mmol). After the



SCHEME 1 Synthesis of twin dimer I, III, and IV series.



SCHEME 2 Synthesis of twin dimer II series.

mixture was stirred for 1 h, chloromethylmethylether (9.0 g, 112.0 mmol) was added dropwise to the mixture under an ice bath. The reaction mixture was stirred for 13 h at room temperature. After the reaction mixture was poured into water, the aqueous mixture was extracted with ethyl acetate. The ethyl acetate solution was dried over magnesium sulfate. The ethyl acetate was evaporated under reduced pressure. The yellow liquid was obtained in an 89.9% yield (6.7 g) and was used without further purification.

$^1\text{H-NMR}$ (CDCl_3) δ ppm: 3.5 (s, 3H, CH_3), 5.5 (s, 2H, CH_2), 7.2 (d, 2H, Ar-H). 7.8 (d, 2H, Ar-H), 9.9 (s, 1H, CHO).

4-hexyloxybenzylcyanide (2)

1-Bromohexane (3.7 g, 23.0 mmol) and potassium carbonate (0.2 g, 68.0 mmol) was added to a dimethylformamide solution (5 ml) of p-hydroxybenzyl cyanide (3.0 g, 23.0 mmol). The reaction mixture was heated at 80°C for 4 h. The mixture was poured into water. The aqueous solution was extracted with chloroform. The chloroform solution was dried over magnesium sulfate. The chloroform was evaporated under reduced pressure. The brownish liquid was obtained in a 95.5% yield (14.3 g) and was used without further purification.

$^1\text{H-NMR}$ (CDCl_3) δ ppm: 0.8 (s, 3H, CH_3), 1.3 (m, 4H, CH_2), 3.7 (s, 2H, CH_2-CN), 4.0 (m, 2H, OCH_2), 6.8 (d, 2H, Ar-H), 7.2 (d, 2H, Ar-H).

4'-(2-methyl-1-butoxy)benzylcyanide (2)

This compound was synthesized according to the synthetic method of the compound (2) by use of 2-methylbutanol tosylate. The crude product was obtained. This compound was used without further purification.

4-Hexyloxy-4'-methoxymethyloxycyanostilbene (3)

Potassium hydroxide (1.2 g, 20.0) was dissolved in ethanol (50 ml). The compound (1) (1.23 g, 8.0 mmol) was added to the ethanol solution. After the compound (2) was added to the ethanol solution with stirring, the reaction mixture was stirred for 4 h at room temperature. The obtained precipitate was washed with an HCl aqueous solution and then was washed with water until a neutral aqueous solution was obtained. The product was purified by recrystallization from methanol and was obtained in a 64.0% yield (1.9 g).

$^1\text{H-NMR}$ (CDCl_3) δ ppm: 0.8 (t, 3H, CH_3), 1.3–1.9 (m, 6H, CH_2), 3.5 (s, 3H, OCH_3), 4.0 (m, 2H, OCH_2), 5.5 (s, 2H, OCH_2), 6.8 (d, 2H, Ar-H), 7.1 (d, 2H, Ar-H), 7.6 (d, 2H, Ar-H), 7.8 (d, 2H, Ar-H).

4-Hexyloxy-4'-hydroxycyanostilbene (4)

The compound (3) was added to the mixture of methanol and 2N HCl aqueous solution. Then tetrahydrofuran was added to the mixture to dissolve the compound (3). The reaction mixture was stirred for 12 h at 50°C. An aqueous solution of sodium hydrogen carbonate was added to the reaction mixture, and then the aqueous solution was extracted with diethyl ether. The diethyl ether was evaporated to dryness. The yellow solid was purified by recrystallization from methanol and was obtained in an 88.0% yield (1.1 g).

$^1\text{H-NMR}$ (CDCl_3) δ ppm: 0.8 (t, 3H, CH_3), 1.3–1.9 (m, 6H, CH_2), 4.0 (m, 2H, OCH_2), 6.8 (m, 4H, Ar-H), 7.4 (s, 1H, CH=), 7.6 (d, 2H, Ar-H), 7.8 (d, 2H, Ar-H). IR (nujol) ν cm^{-1} : 3297 (OH, phenol), 2229 (CN), 1605 and 1508 (aromatic group).

4-(2-methylbutoxy)-4'-hydroxycyanostilbene (4)

This compound was synthesized according to the same procedure as synthetic method of 4-hexyloxy-4'-hydroxycyanostilbene.

$^1\text{H-NMR}$ (CDCl_3) δ ppm: 1.0 (m, 6H, CH_3), 1.2–1.3 (m, 1H, CH), 1.5–1.6 (m, 1H, CH_2), 1.8–1.9 (m, 1H, CH_2), 3.7–3.8 (m, 2H, OCH_2), 6.0 (s, 1H, OH), 6.9 (d, 4H, Ar-H), 7.4 (s, 1H, CH=), 7.6 (d, 2H, Ar-H), 7.8 (d, 2H, Ar-H).

Twin Dimer I (n = 6): TD-I-6

The compound (4) (1.1 g, 1.0 mmol) was dissolved in tetrahydrofuran (30 ml). Triethylamine (0.9 g, 8.6 mmol) was added to the tetrahydrofuran solution. A tetrahydrofuran solution (30 ml) of suberoyl chloride (0.6 g, 2.9 mmol) was added dropwise to the tetrahydrofuran solution of the compound (4) and triethylamine. The reaction mixture was stirred for 24 h at room temperature. The tetrahydrofuran was evaporated to dryness. The

residue was washed with an HCl aqueous solution and then was washed with water until a neutral aqueous solution was obtained. The product was purified by recrystallization twice from a mixed solvent (methanol/chloroform = 1/1). The white solid was obtained in a 58.5% (0.79 g).

$^1\text{H-NMR}$ (CDCl_3) δ ppm: 0.9 (t, 6H, CH_3), 1.3–1.9 (m, 24H, CH_2), 2.6 (t, 4H, OOCCH_2), 4.0 (t, 4H, OCH_2), 6.8 (d, 4H, Ar-H), 7.1 (d, 4H, Ar-H), 7.4 (s, 2H, $\text{CH}=\text{}$), 7.6 (d, 4H, Ar-H), 7.8 (d, 4H, Ar-H).

Twin Dimer II (n = 6): TD-II-6

The twin dimer was obtained using the compound (1) in Scheme 2 according to our literature [14]. The yellow product was obtained in a 36.4% yield. NMR and Fourier transform infrared (FTIR) measurements supported the finding that synthesized twin dimers had desirable chemical structures.

Characterization

$^1\text{H-NMR}$ was carried out with a JEOL JNM-LA 400 spectrometer using CDCl_3 as the solvent. Infrared spectra were recorded on a JEOL JIR 7000 spectrometer. Spectra were collected at 4 cm^{-1} resolution. DSC measurements were conducted with a Mettler DSC821^e. Optical microscopy was performed on a Nikon polarizing optical microscope, OPTIPHOTO-POL, equipped with a Mettler FP80 controller and a FP82 hot stage. Thermal properties of synthesized materials were investigated by optical microscopy and DSC measurements. X-ray diffraction patterns were recorded with a RIGAKU RINT2500 with Ni-Filtered $\text{CuK}\alpha$ radiation. The sample in quartz capillary (diameter 1 mm) was held in a temperature-controlled cell (RIGAKU LC high-temperature controller). Mesomorphic structure of twin dimers was investigated by X-ray measurements. UV-vis-NIR spectroscopy measurements were carried out with a HITACHI U-3410 spectrophotometer.

RESULTS AND DISCUSSION

In our previous work, we found that the linking group between the mesogenic group and the flexible spacer, as well as the position of the cyano group in the mesogenic group, played an important role for the exhibition of mesophases for twin dimers (TDs) containing cyanostilbene moieties [14]. In this study, to clarify the influence of the terminal group of TDs containing cyanostilbene moieties, we synthesized TDs containing cyanostilbene moieties with different terminal chain lengths, different flexible spacer lengths, or both, as shown in Figure 2. Thermal properties of the

TDs were investigated by polarizing optical microscopy and differential scanning calorimetry (DSC) measurements. Mesomorphic phase structures of TDs were investigated by X-ray measurements.

Figure 3 shows DSC curves of TD-I-6 with ester linking group between the mesogenic group and the flexible spacer. Three peaks are detected on both heating and cooling scans of TD-I series. The peaks at 93°C and at 167°C on heating scan are assigned to the melting and clearing temperatures, respectively. This assignment is supported by observation of the optical texture of TD-I-6. A schlieren texture was observed in the temperature range between melting and clearing points. TD-I-6 displays two mesophases in the temperature range between melting and clearing points.

Figure 4 shows X-ray patterns of TD-I-6. A sharp peak in the small-angle region and a broad peak in the wide-angle region are observed in the X-ray pattern of TD-I-6 at 105°C. A d-spacing based upon the sharp peak in the small-angle region is 43 Å, while the calculated molecular length of the TD is 49 Å. The structure of the mesophase in the lower mesomorphic temperature range would be a smectic C phase due to observation of a schlieren texture and the X-ray pattern for the twin dimer, while in the higher mesomorphic temperature range a broad peak in the wide-angle region is detected in the X-ray pattern of TD-I-6. The phase structure of TD-I-6 in

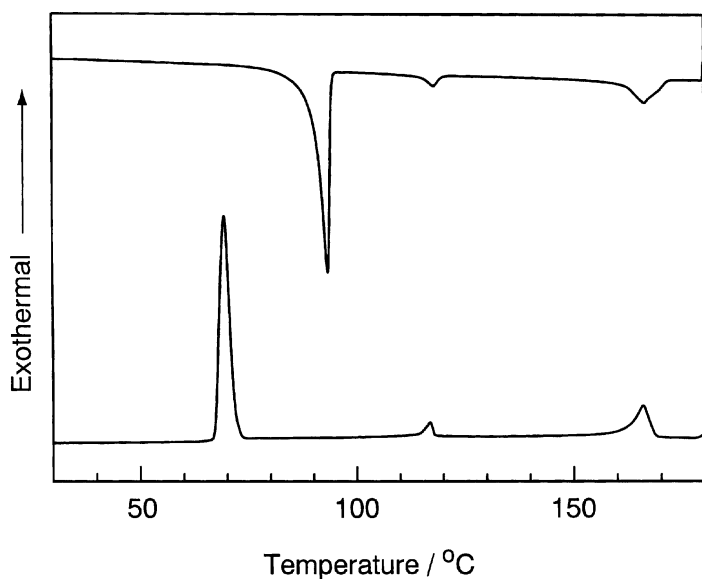


FIGURE 3 DSC curves of TD-I-6.

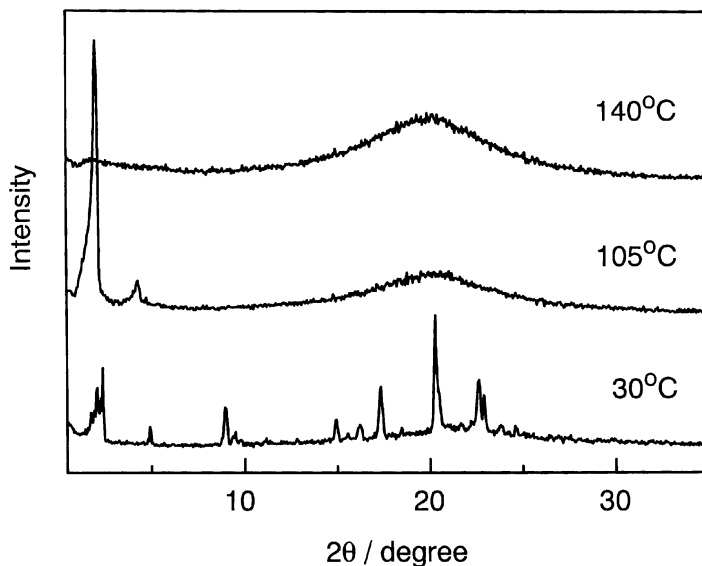


FIGURE 4 X-ray patterns of TD-I-6.

the higher mesomorphic temperature range is a nematic phase based upon observation of the schlieren texture and this X-ray pattern.

The X-ray pattern of TD-I-3 at 115°C on heating scan was similar to that of TD-I-6 at 105°C as shown in Figure 4. The d-spacing of TD-I-3 due to the sharp peak in the small-angle region is 39 Å, while the calculated molecular length of TD-I-3 with all-trans conformation is 41 Å. The layer spacing is slightly shorter than that of the calculated molecular length of TD-I-3. In the lower mesomorphic temperature range (109°C–126°C on heating scan) at TD-I-3, initially the optical texture similar to a focal conic texture was observed at 115°C on heating scan; however, annealing of the sample in the lower mesomorphic temperature range led to the appearance of a schlieren texture. Therefore, we determined that the phase structure of TD-I-3 in the lower mesomorphic temperature range was a smectic C phase, although at the present time we cannot clarify the reason why the change in the optical texture of TD-I-3 was induced by annealing in the lower mesomorphic temperature range.

In the X-ray pattern of TD-I series with relatively shorter spacer in higher mesomorphic temperature range, a peak in both the small-angle and the wide-angle regions of TD-I-3 and TD-I-4 was detected. This X-ray pattern of TD-I series with shorter spacer was similar to that observed in the lower mesomorphic temperature range of TD-I-6, although the peak in the small-angle region was very small. The layer structure of

the smectic phase would become loose because the intensity of the peak in the small-angle region was weak compared with that detected in the smectic C phase. In the higher mesomorphic temperature range of TD-I series with relatively shorter spacer, the phase structure would be a cybotactic nematic phase due to the observation of a schlieren texture and the X-ray pattern similar to the smectic phase [15–18].

Thermal properties of TD-I series are summarized in Table 1. Smectic C and nematic phases are observed for TD-I-3, TD-I-4, and TD-I-6. On the other hand, an optical texture characteristic of typical liquid crystals could not be observed in the lower mesomorphic temperature range between 87°C and 50°C on cooling scan of TD-I-5, although birefringence was shown in this temperature range. DSC curves of TD-I-5 are shown in Figure 5. The phase transition enthalpy change at 87°C on cooling scan was 0.7 Jg⁻¹. The value of the enthalpy change would be too small for crystallization. We detected the exothermal peak at 50°C in the DSC curve of TD-I-5 on cooling scan. The peak was attributed to the crystallization of TD-I-5. The DSC curve of TD-I-5 on cooling scan supported that the phase structure in the temperature range between 87°C and 50°C would not be crystal but a mesophase: however, X-ray patterns of TD-I-5 in the lower mesomorphic temperature range were similar to that of a crystal. Therefore, at the present time we cannot clarify the phase structure in the lower mesomorphic temperature range of TD-I-5 on cooling scan. TD-I series

TABLE 1 Phase Transition Temperatures and Entropy Changes from a Nematic Phase to the Isotropic Melt of Twin Dimer I Series

n	Phase transition temperatures/°C	ΔS_{NI} (Jmol ⁻¹ K ⁻¹)
3	$\text{Cr} \xrightleftharpoons[68]{74} \text{Cr}^i \xrightleftharpoons[88]{99} \text{Cr}^{ii} \xrightleftharpoons[126]{109} \text{SmC} \xrightleftharpoons[144]{126} \text{N} \xrightleftharpoons[144]{144} \text{I}$	3.8 (4.0)
4	$\text{Cr} \xrightleftharpoons[73]{109} \text{Cr}^i \xrightleftharpoons[85]{128} \text{SmC} \xrightleftharpoons[143]{148} \text{N} \xrightleftharpoons[185]{186} \text{I}$	9.5 (10.8)
5	$\text{Cr} \xrightleftharpoons[50]{73} \text{Cr}^i \xrightleftharpoons[87]{87} \text{M} \xrightleftharpoons[140]{140} \text{N} \xrightleftharpoons[140]{140} \text{I}$	3.1 (3.0)
6	$\text{Cr} \xrightleftharpoons[69]{93} \text{SmC} \xrightleftharpoons[117]{118} \text{N} \xrightleftharpoons[166]{167} \text{I}$	11.1 (13.2)

Cr, Crⁱ crystal; SmC, smectic C phase; N, nematic phase; M, mesophase; I, isotropic phase; ΔS_{NI} , entropy change from a mesophase to the isotropic melt on cooling scan.

Parentheses () denote ΔS_{NI} on heating scan.

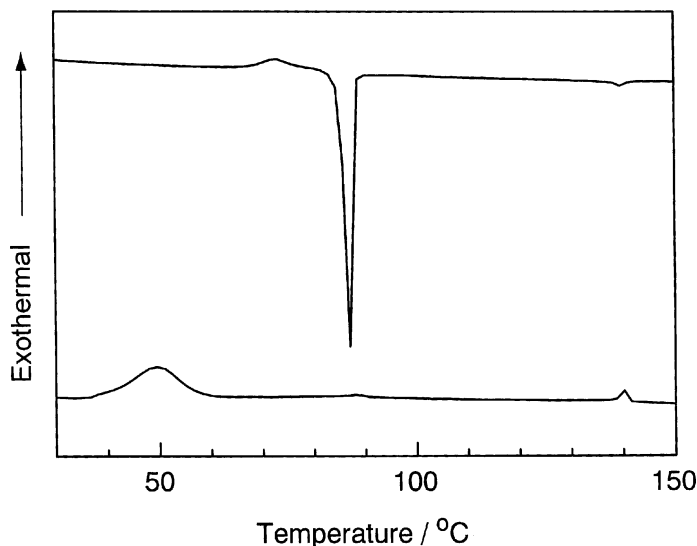


FIGURE 5 DSC curves of TD-I-5.

displayed a remarkable odd–even effect on phase transition temperatures and entropy changes from a nematic phase to the isotropic melt (ΔS_{NI}).

We also synthesized TD-II series with the ether linking group and the flexible spacer to clarify the effect of the linking group on the mesomorphic properties of TDs. A schlieren texture was observed for TD-II-4. DSC curves and X-ray patterns of TD-II-4 are shown in Figure 6 and 7, respectively. TD-II-4 displayed two mesophases in the temperature range between 149 and 179°C on heating scan. The d-spacing of TD-II-4 was 42 Å based on the peak in the small-angle region of the X-ray pattern at 158°C, while the calculated molecular length of TD-II-4 was 45 Å. Therefore, the phase structure in the lower mesomorphic temperature range of TD-II-4 would be a smectic C phase. In the higher mesomorphic temperature range, a cybotactic nematic phase would be shown due to observation of the schlieren texture and a weak peak in the small-angle region of the X-ray pattern, as shown in Figure 7. A cybotactic nematic phase was also observed in the higher mesomorphic temperature range of TD-II-5. Thermal behavior of TD-II series with ether linking group is summarized in Table 2. It would be difficult to exhibit a smectic phase for TD-II series compared to TD-I series with ester linking group.

TD-II series displayed a remarkable odd–even effect on phase transition temperatures and ΔS_{NI} . TD-I series easily exhibited the liquid crystalline phases compared to TD-II series. Therefore, we synthesized TD-III series

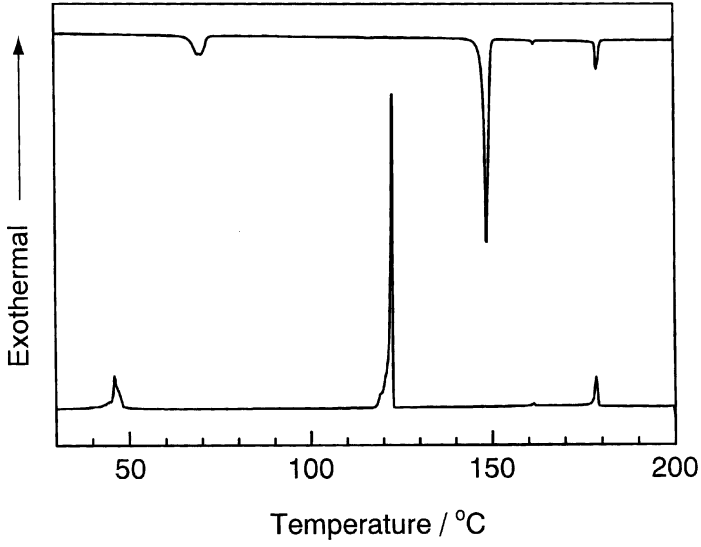


FIGURE 6 DSC curves of TD-II-4.

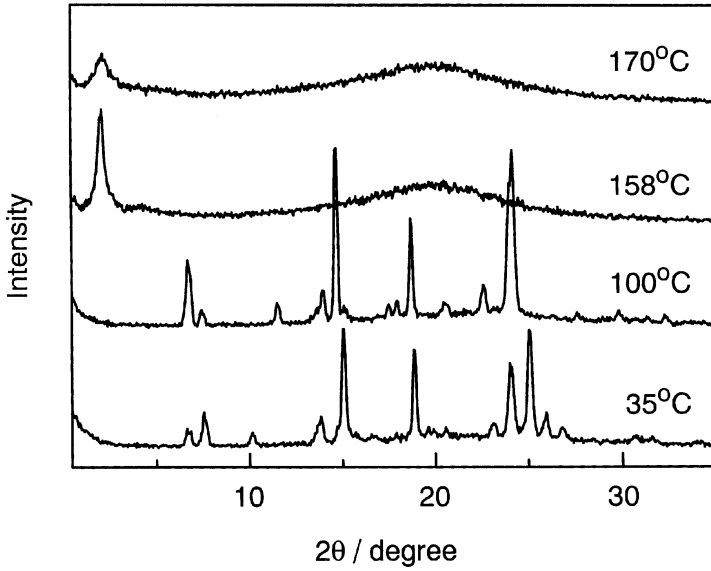


FIGURE 7 X-ray patterns of TD-II-4.

TABLE 2 Phase Transition Temperatures and Entropy Changes from a Nematic Phase to the Isotropic Melt of Twin Dimer II Series

n	Phase transition temperatures/ $^{\circ}\text{C}$	ΔS_{NI} (Jmol $^{-1}$ K $^{-1}$)
3	$\text{Cr} \begin{array}{c} \xrightarrow{89} \\ \xleftarrow{82} \end{array} \text{M} \begin{array}{c} \xleftarrow{94} \\ \xrightarrow{94} \end{array} \text{Cr}^{\text{I}} \begin{array}{c} \xrightarrow{137} \\ \xleftarrow{98} \end{array} \text{N} \begin{array}{c} \xrightarrow{137} \\ \xleftarrow{98} \end{array} \text{I}$	3.8
4	$\text{Cr} \begin{array}{c} \xrightarrow{70} \\ \xleftarrow{46} \end{array} \text{Cr}^{\text{I}} \begin{array}{c} \xrightarrow{149} \\ \xleftarrow{123} \end{array} \text{SmC} \begin{array}{c} \xrightarrow{162} \\ \xleftarrow{161} \end{array} \text{N} \begin{array}{c} \xrightarrow{179} \\ \xleftarrow{179} \end{array} \text{I}$	12.4 (12.3)
5	$\text{Cr} \begin{array}{c} \xrightarrow{100} \\ \xleftarrow{77} \end{array} \text{M} \begin{array}{c} \xrightarrow{101} \\ \xleftarrow{101} \end{array} \text{N} \begin{array}{c} \xrightarrow{118} \\ \xleftarrow{118} \end{array} \text{I}$	4.1 (4.1)
6	$\text{Cr} \begin{array}{c} \xrightarrow{113} \\ \xleftarrow{112} \end{array} \text{Cr}^{\text{I}} \begin{array}{c} \xrightarrow{140} \\ \xleftarrow{126} \end{array} \text{N} \begin{array}{c} \xrightarrow{159} \\ \xleftarrow{159} \end{array} \text{I}$	8.6 (9.0)

Cr, Cr', crystal; Smc, smectic C phase; N, nematic phase; M, mesophase; I, isotropic phase; ΔS_{NI} , entropy change from a mesophase to the isotropic melt on cooling scan.

Parentheses () denote ΔS_{NI} on heating scan.

with different terminal chain length to investigate the effect of the terminal chain length on the thermal behavior of TDs with ester linking group. Here we fixed the length of methylene spacer, because TD-I-6 displayed liquid crystalline phases and simple thermal behavior without a recrystallization.

Phase transition temperatures and ΔS_{NI} for TD-III series are summarized in Table 3. TD-III, with a relatively short terminal chain, showed an enantiotropic nematic phase, while TD-III-6 and TD-III-7, with longer terminal chains, displayed an enantiotropic smectic phase. This is conventional thermal behavior for low molar mass liquid crystals. The temperature range of the smectic phase for TD-III-7 was wider than that of TD-III-6. Terminal chain length played an important role in the exhibition of a smectic phase and the stability of the smectic phase for TDs. In the higher mesomorphic temperature range of TD-III-7, a cybotactic nematic phase was observed.

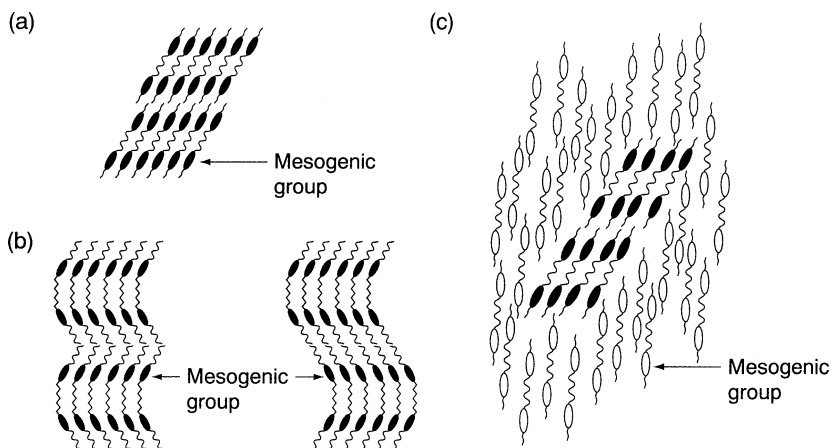
The possible packing models for the smectic C and cybotactic nematic phase of TD series are shown in Figure 8. The models were proposed assuming that TDs form all-trans conformation. Figure 8(a) displays the packing model for the smectic C phase of TD series with even-numbered flexible spacer such as TD-I-4, TD-I-6, TD-II-4, TD-III-6, and TD-III-7. The mesogenic groups of the even-numbered TD series can be parallel to each other. On the other hand, Figure 8(b) shows the packing models for the smectic C phase of TD-I-3 that have odd-numbered flexible spacer. TD-I-3 must have a bent conformation assuming that it forms all-trans conformation. The mesogenic groups of TD-I-3 can be tilted to each other

TABLE 3 Phase Transition Temperatures and Entropy Changes from a Nematic Phase to the Isotropic Melt of Twin Dimer III Series

m	Phase transition temperatures/ $^{\circ}\text{C}$	$\Delta S_{\text{NI}}/(\text{Jmol}^{-1}\text{K}^{-1})$
3	$\text{Cr} \begin{array}{c} \xrightarrow{142} \\ \xleftarrow{126} \end{array} \text{N} \begin{array}{c} \xrightarrow{191} \\ \xleftarrow{189} \end{array} \text{I}$	11.7 (11.9)
4	$\text{Cr} \begin{array}{c} \xrightarrow{165} \\ \xleftarrow{139} \end{array} \text{N} \begin{array}{c} \xrightarrow{186} \\ \xleftarrow{186} \end{array} \text{I}$	12.6 (12.2)
5	$\text{Cr} \begin{array}{c} \xrightarrow{150} \\ \xleftarrow{137} \end{array} \text{N} \begin{array}{c} \xrightarrow{173} \\ \xleftarrow{172} \end{array} \text{I}$	11.6 (11.6)
6	$\text{Cr} \begin{array}{c} \xrightarrow{93} \\ \xleftarrow{69} \end{array} \text{SmC} \begin{array}{c} \xrightarrow{118} \\ \xleftarrow{117} \end{array} \text{N} \begin{array}{c} \xrightarrow{167} \\ \xleftarrow{166} \end{array} \text{I}$	11.1 (13.2)
7	$\text{Cr} \begin{array}{c} \xrightarrow{98} \\ \xleftarrow{77} \end{array} \text{SmC} \begin{array}{c} \xrightarrow{145} \\ \xleftarrow{145} \end{array} \text{N} \begin{array}{c} \xrightarrow{166} \\ \xleftarrow{166} \end{array} \text{I}$	14.2 (13.4)

Cr, crystal; SmC, smectic C phase; N, nematic phase; I, isotropic phase; ΔS_{NI} , entropy change from a mesophase to the isotropic melt on cooling scan.

Parentheses () denote ΔS_{NI} on heating scan.

**FIGURE 8** Possible packing models for smectic C and cybotactic nematic phases of twin dimers: (a) smectic C phase for twin dimers with even-numbered flexible spacer, (b) smectic C phase of TD-I-3, (c) cybotactic nematic phase.

[12,13]. Figure 8(c) indicates one of the models for the molecular array in the cybotactic nematic phase. The cybotactic nematic phase has the molecular array with smectic C order (cybotactic group) in nematic molecular array. The cybotactic group in the nematic structure is a cluster of liquid crystal (LC) molecules that form the molecular array similar to the smectic C phase. Both the conventional nematic array of LC molecules and the cybotactic groups coexist in the cybotactic nematic phase [15–18].

Furthermore, to investigate the effect of an optical active moiety on the thermal behavior of TDs, we synthesized TD-IV series, which had an optical active terminal chain and different flexible spacer lengths. Phase transition temperatures, entropy changes from mesophase to isotropic phase (ΔS_{MI}), and optical rotation of TD-IV series are summarized in Table 4. It does not seem easy for TD-IV series to show enantiotropic mesophases. In DSC curves of TD-IV-4, two peaks (at 125 and 155°C) were observed on the heating scan, while three peaks (at 155, 122, and 108°C) were shown on the cooling scan. The two peaks on the heating scan were assigned to the melting and clearing temperatures, respectively, based upon the polarized optical microscopy observation. While the three peaks on the cooling scan were attributed to the clearing, mesophase–mesophase transition and melting temperatures, respectively. An oily streak texture was observed in the temperature range between 125 and 155°C on the heating scan and

TABLE 4 Phase Transition Temperatures, Entropy Changes from a Mesophase to the Isotropic Melt, and Optical Rotation of Twin Dimer IV Series

n	Phase transition temperatures/°C	$[\alpha]^{25}_D$	$\Delta S_{MI}/(\text{Jmol}^{-1}\text{K}^{-1})$
3	Cr $\xrightleftharpoons[99]{145}$ I	43.3	—
4	Cr $\xrightleftharpoons[108]{125}$ Sm $\xrightleftharpoons[122]{125}$ Ch $\xrightleftharpoons[155]{155}$ I	16.5	8.7 (8.1)
5	Cr $\xrightleftharpoons[70]{125}$ M $\xrightleftharpoons[85]{125}$ I	50.7	1.6
6	Cr $\xrightleftharpoons[95]{140}$ Ch $\xrightleftharpoons[133]{140}$ I	25.5	9.7
7	Cr $\xrightleftharpoons[52]{72}$ Cr' $\xrightleftharpoons[M]{77}$ Cr'' $\xrightleftharpoons[82]{100}$ I	49.3	2.2

Cr, Cr', crystal; Sm, smectic phase; Ch, cholesteric phase; M, mesophase; I, isotropic phase, ΔS_{MI} , entropy change from a mesophase to the isotropic melt on cooling scan.

Parentheses () denote ΔS_{MI} on heating scan.

between 155 and 122°C on cooling scan. This microscopy observation supported that TD-IV-4 displayed an enantiotropic cholesteric phase.

Oily streak textures of cholesteric phases can be observed when the helical axis of cholesteric helical structure is perpendicular to the glass plate. We cannot estimate the helical pitch of TD-IV-4 from the optical texture. The selective reflection wavelength is related to the helical pitch of cholesteric helical structures. Therefore we investigated the selective reflection wavelength of cholesteric structures for TD-IV-4 and TD-IV-6 by UV-vis-NIR spectroscopy measurements. Transmittance spectra of TD-IV-6 are shown in Figure 9. The selective reflection wavelengths of cholesteric structures were about 880 nm at 140°C for TD-IV-4 and about 900 nm at 120°C for TD-IV-6, respectively. The selective reflection peak for TD-IV-4 and TD-IV-6 was slightly shifted to a shorter wavelength with decreasing temperature.

Figure 10 shows the X-ray patterns of TD-IV-4 at 115°C on the cooling scan. A sharp peak in the small-angle region and a broad peak in the wide-angle region were observed in the X-ray pattern of TD-IV-4. The d-spacing of TD-IV-4 was 35 Å due to the sharp peak in the small-angle

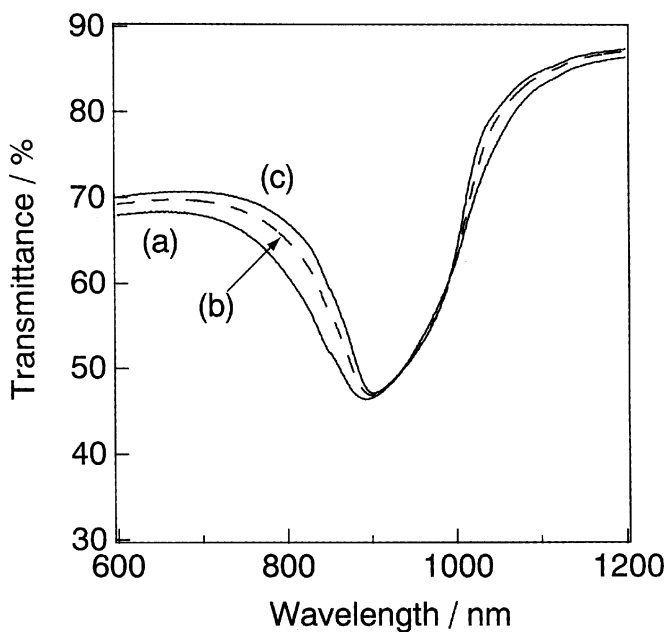


FIGURE 9 Transmittance spectra of planar-oriented samples of TD-IV-6 at (a) 110°C, (b) 115°C, and (c) 120°C.

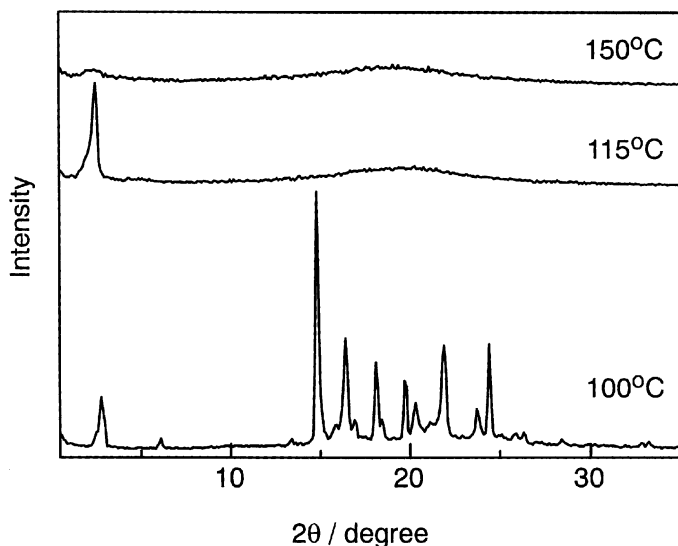


FIGURE 10 X-ray patterns of TD-IV-4.

region, while the calculated molecular length of TD-IV-4 with all-trans conformation was about 41 Å. The d-spacing obtained was shorter than that of the calculated molecular length. Therefore, we expected that the phase structure in the lower mesomorphic temperature range would be a smectic C* phase; however, a clear optical texture characteristic of smectic C* phase was not observed, but birefringence was observed in the lower mesomorphic temperature range of TD-IV-4.

A remarkable odd–even effect on ΔS_{MI} on cooling scan was observed for TD-IV series. TD-IV-even number series showed a cholesteric phase, while TD-IV-odd number series did not exhibit a typical liquid crystalline phase. This thermal behavior would originate from the difference in the orientation of mesogenic groups based upon the flexible spacer length. Birefringence was observed in the temperature range of TD-IV-odd number series; however, we detected the crystallization of TD-IV-odd number series under annealing by optical microscopy measurements. We did not observe a typical X-ray pattern for liquid crystalline phase, but an X-ray pattern characteristic of a crystalline phase. In the X-ray pattern, many sharp peaks were observed in the wide angle region. Crystallization would occur during the X-ray measurements of TD-IV-odd number series. The monotropic mesophase on cooling scan would be unstable thermodynamically, and phase transition from mesophase to crystal would occur under annealing.

CONCLUSIONS

We synthesized twin dimers (TDs) with different linking group between a mesogenic group and a flexible spacer, different spacer length, and different terminal alkyl chain length. Liquid crystallinity of TDs with ester linking group was superior to that of TDs with ether linking group, although we cannot clarify the origin of the difference in liquid crystallinity between TDs with ester or ether linking group. A remarkable odd–even effect on the phase transition temperatures and nematic–isotropic phase transition entropy changes was observed for the TDs with different spacer length. In contrast, length of terminal group played an important role in exhibiting a smectic phase for TDs with an ester linking group. A clear odd–even effect on the phase transition temperatures and nematic–isotropic phase transition entropy changes was not detected for the TDs with different lengths of terminal group. The exhibition of cholesteric phase for TDs with optically active terminal moiety was dependent upon the flexible spacer length.

REFERENCES

- [1] Ciferri, A., Krigbaum, W. R., & Meyer, R. B. (Eds.). (1982). *Polymer Liquid Crystals* (Academic Press), London.
- [2] Buglione, J. A., Roviello, A., & Sirigu, A. (1984). *Mol. Cryst. Liq. Cryst.*, 106, 169–185.
- [3] Abe, A. & Furuya, H. (1986). *Kobunshi Ronbunshu*, 43, 247–252.
- [4] Barnes, P. J., Douglass, A. G., Heeks, S. K., & Luckhurst, G. R. (1993). *Liq. Cryst.*, 13, 603–613.
- [5] Luckhurst, G. R. (1995). *Macromol. Symp.*, 96, 1–26.
- [6] Marcellis, A. T. M., Koudijs, A., & Sudhölter, E. J. R. (1995). *Liq. Cryst.*, 18, 843–850.
- [7] Date, R. W., Imrie, C. T., Luckhurst, G. R., & Seddon, J. M. (1992). *Liq. Cryst.*, 12, 203–238.
- [8] Blatch, A. E. & Luckhurst, G. R. (2000). *Liq. Cryst.*, 27, 775–787.
- [9] Hogan, J. L., Imrie, C. T., & Luckhurst, G. R. (1988). *Liq. Cryst.*, 3, 645–650.
- [10] Attard, G. S., Date, R. W., Imrie, C. T., Luckhurst, G. R., Roskilly, S. J., & Taylor, L. (1994). *Liq. Cryst.*, 16, 529–581.
- [11] Henderson, P. A., Niemeyer, O., & Imrie, C. T. (2001). *Liq. Cryst.*, 28, 463–472.
- [12] Watanabe, J., Komura, H., & Niiori, T. (1993). *Liq. Cryst.*, 13, 455–465.
- [13] Watanabe, J., Niiori, T., Choi, S.-W., Takanishi, Y., & Takezoe, H. (1998). *Jpn. J. Appl. Phys.*, 37, L401–L403.
- [14] Aoki, H., Mihara, T., & Koide, N. (2004). *Mol. Cryst. Liq. Cryst.*, 408, 53–70.
- [15] Kelker, H., & Hatz, R. (Eds.). (1980). *Handbook of Liquid Crystals* (Verlag Chemie) pp. 5, 26.
- [16] de Vries, A. (1970). *Mol. Cryst. Liq. Cryst.*, 10, 219–236.
- [17] Blumstein, A., Vilasagar, S., Ponrathnam, S., Clough, S. B., & Blumstein, R. B. (1982). *J. Polym. Sci.: Polymer Phys. Edn.*, 20, 877–892.
- [18] Azároff, L. V. & Schuman, C. A. (1985). *Mol. Cryst. Liq. Cryst.*, 122, 309–319.